

# Brain Neuroplastic Changes Accompany Anxiety and Memory Deficits in a Model of Complex Regional Pain Syndrome

Maral Tajerian, Ph.D., David Leu, M.Sc., Yani Zou, Ph.D., Peyman Sahbaie, M.D., Wenwu Li, Ph.D., Hamda Khan, Vivian Hsu, Wade Kingery, Ph.D., Ting Ting Huang, Ph.D., Lino Becerra, Ph.D., J. David Clark, M.D., Ph.D.

## ABSTRACT

**Background:** Complex regional pain syndrome (CRPS) is a painful condition with approximately 50,000 annual new cases in the United States. It is a major cause of work-related disability, chronic pain after limb fractures, and persistent pain after extremity surgery. Additionally, CRPS patients often experience cognitive changes, anxiety, and depression. The supraspinal mechanisms linked to these CRPS-related comorbidities remain poorly understood.

**Methods:** The authors used a previously characterized mouse model of tibia fracture/cast immobilization showing the principal stigmata of CRPS ( $n = 8$  to 20 per group) observed in humans. The central hypothesis was that fracture/cast mice manifest changes in measures of thigmotaxis (indicative of anxiety) and working memory reflected in neuroplastic changes in amygdala, perirhinal cortex, and hippocampus.

**Results:** The authors demonstrate that nociceptive sensitization in these mice is accompanied by altered thigmotactic behaviors in the zero maze but not open field assay, and working memory dysfunction in novel object recognition and social memory but not in novel location recognition. Furthermore, the authors found evidence of structural changes and synaptic plasticity including changes in dendritic architecture and decreased levels of synaptophysin and brain-derived neurotrophic factor in specific brain regions.

**Conclusions:** The study findings provide novel observations regarding behavioral changes and brain plasticity in a mouse model of CRPS. In addition to elucidating some of the supraspinal correlates of the syndrome, this work supports the potential use of therapeutic interventions that not only directly target sensory input and other peripheral mechanisms, but also attempt to ameliorate the broader pain experience by modifying its associated cognitive and emotional comorbidities. (**ANESTHESIOLOGY 2014; 121:852-65**)

**C**OMPLEX regional pain syndrome (CRPS) is a painful, disabling, and often chronic condition with an estimated 50,000 new cases in the United States each year.<sup>1</sup> It is characterized by severe pain-related changes (allodynia and hyperalgesia), trophic changes (abnormalities in hair and nail growth), neurovascular abnormalities (abnormal sweating, edema, and skin discoloration), and motor changes (tremor).<sup>2-4</sup> Despite the fact that CRPS has been a documented clinical entity for at least 150 yr, we have only a partial understanding of the supporting mechanisms, and no broadly effective treatments. Current therapies including physical, interventional, pharmacological, rehabilitative, and alternative are limited in their effectiveness, and none are curative,<sup>5,6</sup> leaving more than 80% of chronic CRPS patients severely disabled.<sup>7</sup>

Similar to other chronic pain conditions, CRPS encompasses neurocognitive changes as well as alterations in mood

### What We Already Know about This Topic

- Chronic regional pain syndrome is associated with cognitive changes, depression, and anxiety, but the mechanisms for these associations are unclear

### What This Article Tells Us That Is New

- In a model of complex regional pain syndrome in mice, the animals became hypersensitive to light touch, but also exhibited behaviors indicative of anxiety and diminished working memory in some tests
- These changes were accompanied by structural changes in several brain regions, suggesting that complex regional pain syndrome can result in broad changes in the central nervous system as well as producing pain

and anxiety that affect quality of life, level of disability, and need for additional health care.<sup>8,9</sup> More broadly, a recent

This article is featured in "This Month in Anesthesiology," page 1A. Corresponding article on p. 675. Supplemental Digital Content is available for this article. Direct URL citations appear in the printed text and are available in both the HTML and PDF versions of this article. Links to the digital files are provided in the HTML text of this article on the Journal's Web site ([www.anesthesiology.org](http://www.anesthesiology.org)).

Submitted for publication February 7, 2014. Accepted for publication June 13, 2014. From the Veterans Affairs Palo Alto Health Care System, Palo Alto, California (M.T., P.S., W.L., H.K., J.D.C.); Department of Anesthesiology, Stanford University School of Medicine, Stanford, California (M.T., P.S., W.L., J.D.C.); Palo Alto Institute of Research and Education, Palo Alto, California (M.T., D.L., Y.Z., H.K., V.H.); Department of Neurology and Neurological Sciences, Stanford University, Stanford, California (Y.Z., T.T.H.); Physical Medicine and Rehabilitation Service, Veterans Affairs Palo Alto Health Care System, Palo Alto, California (W.K.); Geriatrics Research Education and Clinical Center, Veterans Affairs Palo Alto Health Care System, Palo Alto, California (D.L., Y.Z., V.H., T.T.H.); and P.A.I.N. Group, Departments of Anesthesia and Psychiatry, Boston Children's Hospital and Harvard Medical School, Boston, Massachusetts (L.B.).

Copyright © 2014, the American Society of Anesthesiologists, Inc. Lippincott Williams & Wilkins. Anesthesiology 2014; 121:852-65

meta-analysis of 24 separate studies on cognition in pain patients concluded that there was a consistent moderate effect of pain on working memory.<sup>10</sup> In a related study, it was observed that approximately 20% of the new patients to a multidisciplinary pain center showed clinically significant impairment on neurocognitive testing.<sup>11</sup> Although the preponderance of the CRPS literature focuses on peripheral changes that accompany the signs and symptoms of this syndrome, more recent studies have used neuroimaging techniques to study changes within the central nervous system (CNS); the existence of pain-associated cognitive and emotional comorbidities suggests that alterations in brain structure and function may contribute to sustained pain, emotional changes, and neurocognitive features in chronic CRPS patients.<sup>12,13</sup>

Various rodent models that mimic common signs and symptoms observed in human CRPS patients exist. For instance, the chronic postischemic pain model is characterized by chronic mechanical allodynia, microvascular injury, and chronic ischemia,<sup>14</sup> whereas the needlestick distal nerve injury is accompanied by allodynia, dystonia, and epidermal neurite loss<sup>15</sup>, and the focal neuritis model displays changes in sympathetic and sensory neuronal discharge.<sup>16</sup> To better understand the changes in cognition and emotion in CRPS and to examine the structural and biochemical brain correlates of these changes, we utilized a mouse tibial fracture model characterized by nociceptive sensitization, bone demineralization, edema, and warmth similar to the changes found in CRPS I patients.<sup>17–19</sup>

Our primary aim of this study was to measure the behavioral phenotypes of anxiety and memory dysfunction that accompany ongoing mechanical allodynia in our model. These studies were then followed by a second line of investigation to examine the neuroplastic changes that accompany these behavioral phenotypes. To that end, histological analysis of dendritic architecture in addition to the assessment of synaptophysin and brain-derived neurotrophic factor (BDNF) protein levels were performed on tissue from the amygdala, perirhinal cortex, and hippocampus. These three centers have well-established roles in emotional disorders and cognitive difficulties.<sup>20–24</sup>

The results of this study support the hypothesis that common features of chronic CRPS including pain, anxiety, and memory deficits are accompanied by structural and biochemical changes in specific brain centers.

## Materials and Methods

### Animals

A total of four cohorts of mice were used. Male C57/B6J mice aged 12 to 14 weeks were purchased from a commercial supplier (Jackson Labs, Sacramento, CA) and were allowed to habituate to the animal facility for a minimum of 10 days before the experiments. Mice were housed in groups of four on a 12 h light-dark cycle and an ambient temperature of  $22^\circ \pm 3^\circ\text{C}$ , with food and water available *ad libitum*. All

animal procedures and experimental designs were approved by the Veterans Affairs Palo Alto Health Care System Institutional Animal Care and Use Committee (Palo Alto, California) and followed the “animal subjects” guidelines of the International Association for the Study of Pain.

### Limb Fracture and Cast Immobilization

Mice were randomly allocated to the control or the fracture/cast group. Mice were anesthetized with 1.5% isoflurane and underwent a distal tibial fracture in the right leg. In brief, a hemostat was used to make a closed fracture of the right tibia just distal to the middle of the tibia. Then the hind limb was wrapped in casting tape (3M; Scotchcast Plus, St. Paul, MN) so the hip, knee, and ankle were all fixed. The cast extended from the metatarsals of the hind paw up to a spica formed around the abdomen. A window was left open over the dorsal paw and ankle to prevent constriction when postfracture edema developed.<sup>18</sup> After the procedure, the mice were given subcutaneous buprenorphine (0.05 mg/kg) and enrofloxacin (5 mg/kg) for the next 2 days, as well as normal saline (1.5 ml once) for postoperative analgesia, prevention of infection, and dehydration. Mice were inspected daily to ensure the cast was positioned properly through the 3-week period of cast immobilization. Mice were provided with chow pellets postoperatively *ad libitum*; dietary gels were also made available on the cage floor for mice having undergone surgery. At 3 weeks after surgery, the mice were briefly anesthetized using isoflurane and the casts were removed.

Naive age- and sex-matched mice were used as control. We have chosen to use naive mice instead of sham (cast immobilization only) animals because cast immobilization results in an intermediate phenotype that shows signs of transient mechanical allodynia.<sup>17</sup> This is consistent with the clinical situation where limited CRPS-like changes are observed when casts are applied to healthy human limbs.<sup>25</sup> In the tibia fracture/cast immobilization model of CRPS, both the fracture and the immobilization are needed for the sustained, CRPS-like phenotype in mice, and as such, the cast immobilization is a crucial part of the model rather than an inevitable procedure after fracture.

### Behavioral Testing

The experimenter was blind to the identity and experimental condition of the animals throughout the behavioral experiments and data analysis. Mice were habituated to handling by the experimenter for a few minutes each day for 7 days before initiation of the behavioral tests. Each of the two experimental cohorts included 16 (control) and 20 (fracture/cast) animals and, except for mechanical sensitivity, all behavioral tests were carried out 7 weeks after fracture (completed by 9 weeks after fracture) in the following order: open field (OF), novel location recognition (NLR), novel object recognition (NOR), zero maze, and social memory. Eight (control) and 11 (fracture/cast) animals were randomly chosen to be tested at the 14- and 18-week timepoints (see

Supplemental Digital Content 1, <http://links.lww.com/ALN/B71>). Sample size determination was guided by prior experience with these behavioral assays.

Animals were allowed to habituate in their home cages in the experimental room for 1 h before testing. All behavioral studies were carried out in a clean and quiet room. OF, zero maze, NOR, NLR, and social memory tests were recorded and analyzed by TopScan Lite (CleverSys, Reston, VA) in real time.

**Mechanical Hypersensitivity.** Calibrated monofilaments (Stoelting Co., Wood Dale, IL) were applied to the plantar surface of the hind paw and the 50% threshold to withdraw (grams) was calculated as previously described.<sup>26</sup> The stimulus intensity ranged from 0.004 to 1.7 g, corresponding to filament numbers (1.65, 2.36, 2.44, 2.83, 3.22, 3.61, 3.84, 4.08, 4.17, and 4.31). For each animal, the actual filaments used within the aforementioned series were determined based on the lowest filament to evoke a positive response followed by five consecutive stimulations using the up-down method. The filament range and average interval were then incorporated along with the response pattern into each individual threshold calculation. Mechanical sensitivity was assessed on the plantar surface of the left hind paw (response = flexion reflex).

**Open Field.** The OF arena measured 45 × 45 × 45 cm and was made of opaque plastic material. Luminosity inside the OF was measured to be 5 lux. The mice were placed into the arena and allowed to explore for 10 min. Total locomotor activity and the time spent in the central portion (11% of total area) were determined for each mouse. The time spent in the center area was used as an index of thigmotaxis, a measure often used for evaluating general anxiety levels in rodents.<sup>27</sup>

**Zero Maze.** The use of zero maze to measure thigmotaxis, indicative of anxiety, was carried out following previously published methods.<sup>28</sup> The maze has an outer diameter of 24 inches, inner diameter of 20 inches, it is 24 inches above the floor and the closed quadrants have 6-inch tall walls. Luminosity inside the open quadrant was measured to be 20 lux, whereas that inside the closed quadrant was measured to be 10 lux. Mice were placed facing one of the closed quadrants of the elevated zero maze to begin the 5-min test period. Total time spent in open and closed quadrants as well as total distance traveled were recorded.

**NLR and NOR.** Novel location recognition and NOR tests were carried out in the same arena as the one used for the OF test to assess working memory.<sup>29</sup> Exploration behavior was used to assess object location and recognition. Mice were placed into the arena from the middle of the south wall, with the north wall of the arena having a large visual cue (28 cm × 21.5 cm [W × H] sheet with alternating black and white columns [column width = 1.5 cm]). Each mouse was presented with two identical objects (OBJ1 and OBJ2) for 10 min (habituation). The two identical objects were placed side by side with equal distance from the east and west walls and were 30 cm away from the visual cue. The next day, mice were first given three 10-min trials with identical setting as the habituation day and the time spent exploring the objects

was recorded. In the fourth 10-min trial, OBJ1 was moved toward the visual cue (novel location), and the time spent exploring OBJ1 in the new location was recorded. In the fifth 10-min trial, OBJ2 (the familiar object) was replaced by a new object (OBJ3, novel object), and the time spent exploring OBJ3 was recorded. During the intertrial intervals of 5 min, mice were returned to their home cage. Objects were replaced with replicates after each trial, and 4% (vol/vol) acetic acid was used to clean and remove potential odors. Exploration behavior in the first 5 min was used to assess NLR and NOR. For NLR, the data were calculated as exploration ratio of time (seconds) spent exploring object in the novel location *versus* that for exploring object in its original location. The exploration ratio of time spent exploring the novel object *versus* that for exploring the familiar object is calculated in NOR. The exploration ratio for novel and familiar location/object is calculated as  $T_{\text{novel}}/(T_{\text{novel}} + T_{\text{familiar}})$  and  $T_{\text{familiar}}/(T_{\text{novel}} + T_{\text{familiar}})$ , respectively, where T equals time. Mice that consistently failed to explore objects for a minimum of 5 s during the training sessions were excluded (*a priori* exclusion criterion) from the NOR and NLR tests (n = 4).

**Social Memory.** Assessment of social recognition memory was carried out according to previously published methods.<sup>30–32</sup> The social testing apparatus is a rectangular, three-chambered box. Each chamber measures 43 cm × 23 cm × 20 cm (W × H × L) in size (two interaction chambers and one neutral chamber). Dividing walls are made from clear Plexiglas (Taps Plastic, Mountain View, CA), with rectangular openings (10 cm × 5 cm) allowing access into each chamber. In each interaction chamber, a stimulus cage (round wire cage, made in-house) was placed during the social testing. During testing, a “stranger” mouse was placed in one or both stimulus cages. The wire mesh separating the interaction chamber from the stimulus cage allows nose contact between test mouse and stranger mouse, while preventing aggressive interactions and also prevents the “stranger” mouse from initiating the social contact. All test mice were experimentally naive to the social interaction test and were habituated to the test room for at least 30 min before assessment. Stranger mice were male C57BL/6J housed in groups of four per cage and have previously been habituated to the round wire cages 24 to 48 h before testing for 15 min each side (30-min total time). *Adaptation phase:* Baseline adaptation was done by placing the test mouse in the central neutral chamber for a 5-min habituation period, followed by the partitions being raised and allowing the mouse to explore freely all three chambers for a 10-min period. During baseline assessments, there was no “stranger” mouse in either of the stimulus cages. Time spent in each chamber was used as baseline data to assess general activity, willingness to circumnavigate the testing apparatus, and to assure that no mouse exhibited a side preference. Locomotor activity and the total number of entries (transitions between chambers of the apparatus) during the 10-min baseline period were assessed. *Social preference (sociability) test:* After baseline data

collection, each mouse was returned to the neutral central chamber for 5 min with partitions closed. During this time, an unfamiliar mouse (stranger 1) was placed within one of the stimulus cages of the interaction chamber. The “doors” to the partitions were raised, allowing the test mouse to move freely throughout the three chambers for a 10-min test session. Location of the “stranger mouse” was alternated between the left and right stimulus cages on consecutive sessions. Measurements of explorations or sniffing directed toward a “stranger mouse” (nose within 1 cm of the wire mesh and directed toward the stranger mouse) were collected in 5 min time bins. The data for the initial 5 min bin were then compared with exploration and sniffing behavior exhibited by the test mouse toward the empty stimulus cage wire mesh in the second interaction chamber. *Memory testing phase:* At the end of the first 10 min, each mouse was returned to its home cage and tested in a second 10-min session to quantify social memory. A second, unfamiliar mouse (stranger mouse 2) was placed into the previously empty stimulus cage. Stranger 1 and stranger 2 mice originate from different home cages and have never come into physical contact with each other or the test subject. Measurements were collected in an identical manner to the social interaction test. Mice that consistently failed to explore each of the three chambers for a minimum of 90 s (15% of the total test time) during the initial 10-min exploratory period (when no stranger mice is present) were excluded (*a priori* exclusion criterion) from the social preference and social memory tests (n = 4).

### **Brain Histology and Dendritic Analysis**

All analyses were done blind to the identity and experimental condition of the animal/tissue. Mice were randomly chosen from a cohort used for behavioral studies. They were anesthetized by 300 µl of ketamine/xylazine cocktail, followed by transcardiac perfusion with 0.9% saline solution at 7 weeks after injury. After the quick and careful removal from the skull, fresh brains were immersed in 10 ml of Golgi-cox stain for 10 days (room temperature and in the absence of light) and transferred to a solution of 30% sucrose for 3 days at 4°C. Coronal sections were cut at room temperature at 100-µm thickness on a vibratome (Leica VA 1200S; Leica Biosystems, Buffalo Grove, IL) and immersed in 0.3% gelatin before mounting on a slide. The stain was visualized by immersing the tissue in the developing solution for 5 to 10 min. Slides were then rinsed in distilled water, dehydrated through graded ethanol, mounted on slides with permount (SP15; Fisher Scientific, Pittsburgh, PA) mounting medium, and cover slipped.

Brain sections located within bregma -1.2 to -2.2 mm were imaged with a 20× objective at 3 µm steps using bright field imaging on a Zeiss LSM 700 microscope (Thornwood, NY). The Mouse Brain in Stereotaxic Coordinates<sup>33</sup> was used as a guide to select appropriate brain sections and to identify areas covering perirhinal cortex and amygdala. On the one hand, the indentation (rhinal fissure) between the ectorhinal cortex and perirhinal cortex was used as a guide

to draw a 100 µm × 50 µm rectangular box as the perirhinal cortex proper. On the other hand, lateral ventricle was used as a guide to draw a circle of 500 µm in diameter to include lateral, basolateral, and basomedial amygdaloid nuclei. Images were analyzed as a 3 µm-step z-stack of 20 slices (20× objective magnification) using bright field imaging (Zeiss LSM 700).

Only Golgi-stained neurons with completely impregnated dendrites and spines were used. Two images per animal (within the designated boxed areas) were randomly chosen for analysis. All neurons in the selected images were numbered and identified using the “Mark and Count” tool in Image J (Bethesda, MD). Then, 10 IDs were randomly selected for further analysis in each z-stack image. Soma area was quantified using the Image J software. Dendritic length, number, and arborization were measured using manual tracing in Neuron J (Bethesda, MD). Sholl analysis was carried out using Fiji (Bethesda, MD) with the Sholl radius set at 5 µm (see Supplemental Digital Content 2, <http://links.lww.com/ALN/B72>, for an illustration of this method). Because of the dense neuronal population in the hippocampus, Sholl analysis was not possible.

Furthermore, in all three brain regions studied, the total number of neurons and spine density were quantified using the “Mark and Count” tool in Image J. Dendritic spines in the amygdala, perirhinal cortex, and granule cells of the hippocampal dentate gyrus were identified based on specific morphological characteristics as reported previously.<sup>34</sup> To determine spine density, images were acquired with 100× oil lens and secondary dendrites with a minimum of 10 µm in length were sampled. The segment of secondary dendrites within 10 µm of the branching point or 10 µm of dendritic terminals were excluded. Spine density is expressed as number of spines per 10 µm dendrite.

### **Protein Quantification**

All analysis was done blind to the identity and experimental condition of the animal/tissue. A separate cohort of mice was used for the biochemical measurements. Mice were anesthetized (isoflurane) and sacrificed by decapitation at 7 weeks after injury. After the quick and careful removal from the skull, the left amygdala, perirhinal cortex, and hippocampus were extracted according to bregma coordinates and stored at -80°C until use.

**Synaptosome Preparation.** Tissue was homogenized in 1XSyn-PER reagent (87793, Thermo Scientific, Pittsburgh, PA) containing “Halt” protease inhibitor cocktail (Thermo Scientific), centrifuged at 1,000g for 10 min to remove cell debris, and the supernatant was transferred to a new tube where it was centrifuged at 17,500g for 20 min. The pellets, containing synaptosomes, were gently resuspended in 40 µl of the reagent (Syn-PER + “Halt”).

**Two-color Fluorescent Western Blot Analysis.** To assess the protein levels of the synaptophysin (also known as p38 synaptic protein) in our synaptosome preparation, Western

blot analysis was performed according to standard procedures. In brief, after sodium dodecyl sulfate polyacrylamide gel electrophoresis and blotting, proteins on the membranes were detected by overnight incubation at 4°C with the primary antibody (mouse monoclonal antisynaptophysin: 1:2,000; S5768; Sigma, St. Louis, MO) followed by incubation with an IRDye 800CW goat anti-mouse IgG (H + L) (1:20,000; 926-32210; LI-COR Biosciences, Lincoln, NE). β-Actin was used as an internal control and was detected with the mouse monoclonal anti-β-actin antibody (1:5,000, ab6276; Abcam, Cambridge, MA) followed by incubation with an IRDye 680CW goat anti-mouse IgG (H + L) (1:20,000, 926-32220; LI-COR Biosciences). The signals were detected and quantified using *Odyssey* (LI-COR Biosciences).

### Protein Extraction and Enzyme-linked Immunosorbent Assay (ELISA).

Tissues were homogenized using T-PER Protein Extraction Reagent (Thermo Scientific 87793) in the presence of proteinase and phosphatase inhibitors (04906837001; Roche Applied Science, San Francisco, CA) and centrifuged at 12,000g for 2 min at 4°C. Supernatant fractions were then frozen at -80°C until use. An aliquot was subjected to protein assay (500-0001; Bio-Rad, Hercules, CA) to normalize BDNF levels. The mouse BDNF ELISA kit was used per manufacturer's instructions (EK0309; Boster Immunoleader, Pleasanton, CA).

### Statistical Analysis

All data are expressed as mean ± SEM. Analysis of repeated parametric measures was accomplished using a two-way ANOVA followed by Bonferroni testing. For simple comparisons of two groups, a two-tailed Student *t* test was used. Welch's correction was used when the assumption of equal variances was not met. For Sholl analysis, individual two-tailed Student *t* tests were used with the Holm-Sidak method for multiple comparisons. Significance was set at *P* value less than 0.05 (Prism 5; GraphPad Software, La Jolla, CA). Sample size for each experimental endpoint is indicated in the figure legends.

## Results

### Tibia Fracture Is Accompanied by Long-lasting Nociceptive Sensitization in the Injured Limb

Ipsilateral (fig. 1A) and contralateral (fig. 1B) measurements of hind paw mechanical thresholds were performed at 3, 4, 7, 14, and 18 weeks postfracture. Mechanical sensitivity, assessed using Von Frey filaments, demonstrated a significant and persistent reduction in mechanical thresholds—up to 14 weeks postfracture—in the injured limb compared with measurements of the contralateral limb or control nonfractured/noncasted mice (two-way ANOVA [fracture factor *F* value = 27.8] followed by Bonferroni testing). Testing for mechanical sensitivity of the contralateral hind paw failed to demonstrate any significant nociceptive changes across the 18-week time course (fig. 1B) (two-way ANOVA; [fracture factor *F* value = 2.96] followed by Bonferroni testing). Although mechanical sensitivity was measured in all behavioral cohorts, only animals that were randomly chosen (*n* = 8 for control and 11 for fracture) to be tested on the 14- and 18-week timepoints are included in this analysis. Earlier data from our group showed that by 7 weeks the edema and warmth characteristic of acute CRPS found at earlier time points had resolved.<sup>18</sup>

### Fracture/Cast Mice Exhibit Signs of Increased Anxiety Levels in the Zero Maze, but Not OF Assay in the Absence of Motor Impairment

**OF Testing.** Fracture/cast mice did not differ from control in overall motor activity measured by the total distance traveled in the OF apparatus (fig. 2, A and B; two-tailed *t* test, 31.94 ± 2.05 m in control vs. 28.01 ± 1.70 m in fracture/cast mice, *P* = 0.15). Similarly, they did not differ from control in the time spent in the center 11% of the OF (fig. 2C; two-tailed *t* test, 16.63 ± 3.44 s in control vs. 16.76 ± 2.23 s in fracture/cast mice, *P* = 0.98). Furthermore, time in center was not different between the two groups when the central area was designated to be 25% of the total area (two-tailed *t* test, 39.32 ± 5.74 s in controls and 38.03 ± 3.74 s in fracture/cast mice, *P* = 0.88; data not shown).

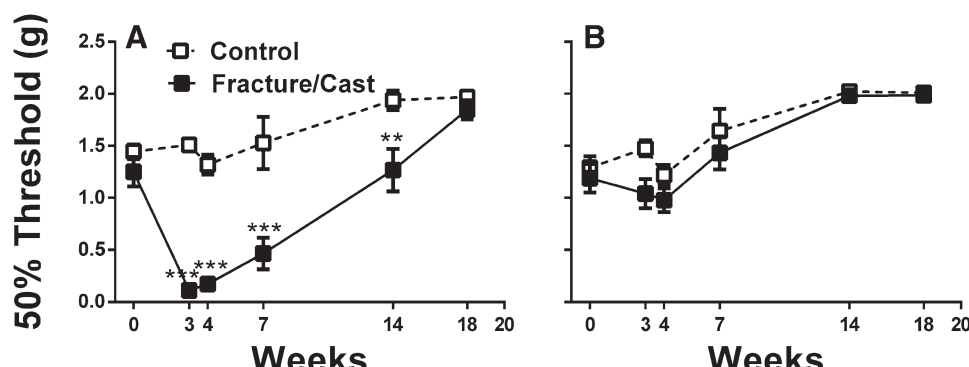


**Fig. 1.** Long-lasting mechanical hypersensitivity in fracture/cast mice. Fracture/cast mice display long-lasting mechanical hypersensitivity on the ipsilateral hind paw 14 weeks after fracture (A). No significant differences in mechanical sensitivity were observed in the contralateral hind paw for any of the groups (B). \*\**P* < 0.01, \*\*\**P* < 0.001. *n* = 8 (control) and *n* = 11 (fracture/cast). Errors bars = SEM.

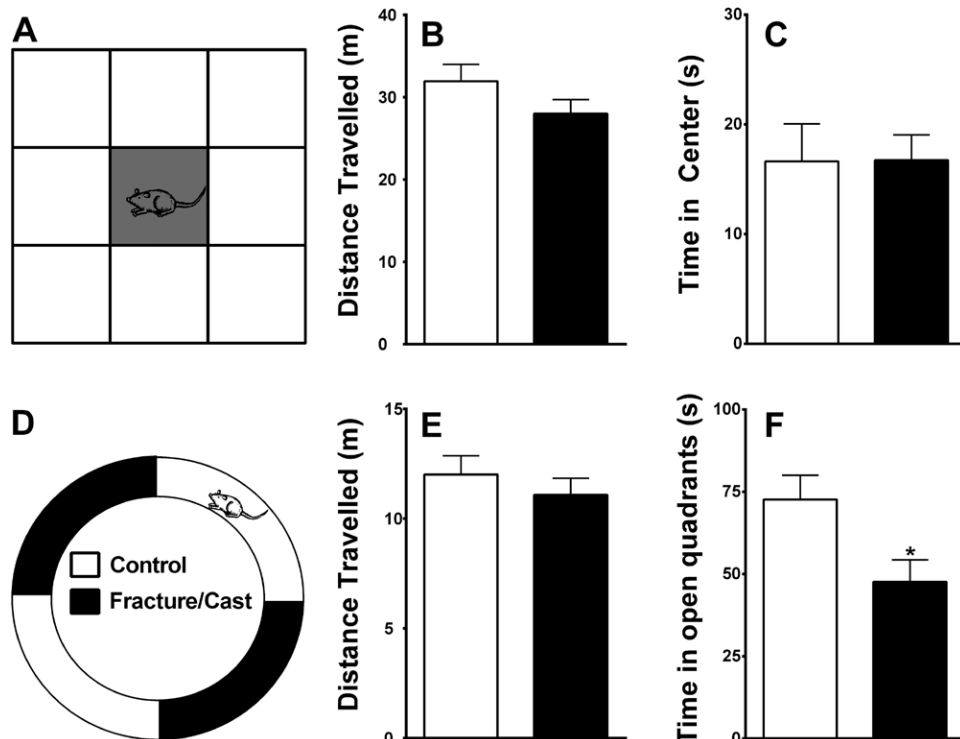


**Fig. 2.** Fracture/cast mice show signs of anxiety. Schematic representation of the open field apparatus highlighting the central square (*A*). Fracture/cast mice neither differ from control mice in the total distance traveled in the open field (*B*) nor do they differ in the time spent in the central square (*C*). Schematic representation of the zero maze apparatus (*D*). Fracture/cast mice do not differ from control mice in the total distance covered in the zero maze (*E*); however, they do differ in the time spent in the open quadrants (*F*). \* $P < 0.05$ .  $n = 16$  per group. Errors bars = SEM.

**Zero Maze Testing.** Consistent with the results obtained from the OF assay, fracture/cast mice did not differ from control in overall motor activity measured by the total distance traveled in the zero maze apparatus (fig. 2, *D* and *E*; two-tailed *t* test,  $12.01 \pm 0.85$  m in control *vs.*  $11.08 \pm 0.76$  m in fracture/cast mice,  $P = 0.42$ ). However, they spent less time in the open quadrants of the zero maze, a measure that is indicative of neophobic anxiety in mice (fig. 2*F*; two-tailed *t* test,  $72.69 \pm 7.36$  s in control *vs.*  $47.67 \pm 6.67$  s in fracture/cast mice,  $P = 0.02$ ).

Example of track images of the OF and zero maze assays can be found in Supplemental Digital Content 3, <http://links.lww.com/ALN/B73>.

#### Fracture/Cast Mice Exhibit Signs of Memory Impairment

**Object Location and Recognition.** Both control and fracture/cast groups performed equally well in the NLR test, as they spent significantly greater time exploring the displaced object compared with the object that was not manipulated (fig. 3, *A* and *B*; two-way ANOVA [fracture factor *F* value approximately 0; object factor *F* value = 45.25] followed by Bonferroni testing). However, compared with control animals, the fracture/cast group performed poorly in the NOR test, as they did not spend more time exploring the novel object compared with the familiar object (fig. 3*C*; two-way ANOVA [fracture factor *F* value approximately 0; object factor *F* value = 45.25] followed by Bonferroni testing).

0; object factor *F* value = 4.65] followed by Bonferroni testing). The failure to differentiate novel from familiar objects is indicative of a working memory deficit.

**Social Memory.** Both control and fracture/cast groups performed equally well in the sociability test (fig. 3*D*), where they spent significantly more time exploring the chamber containing the stranger mouse relative to the chamber with the empty cage (fig. 3*E*; two-way ANOVA [fracture factor *F* value = 0.2; stranger mouse factor *F* value = 54.13] followed by Bonferroni testing). However, the fracture/cast group did not perform as well as the control group in the social memory test. Fracture/cast animals did not spend more time exploring the new stranger mouse, a result that is indicative of diminished social memory (fig. 3*F*; two-way ANOVA [fracture factor *F* value = 0.005; stranger mouse factor *F* value = 15.92] followed by Bonferroni testing).

Example of track images of the NLR, NOR, and social memory assays can be found in Supplemental Digital Content 3, <http://links.lww.com/ALN/B73>.

#### Fracture/Cast Animals Show Altered Dendritic Architecture in the Amygdala

To link the anxiety and memory deficits to structural changes in various brain regions, we quantified dendritic complexity in Golgi-Cox-stained sections. Sholl analysis revealed that, compared with control, fracture/cast mice

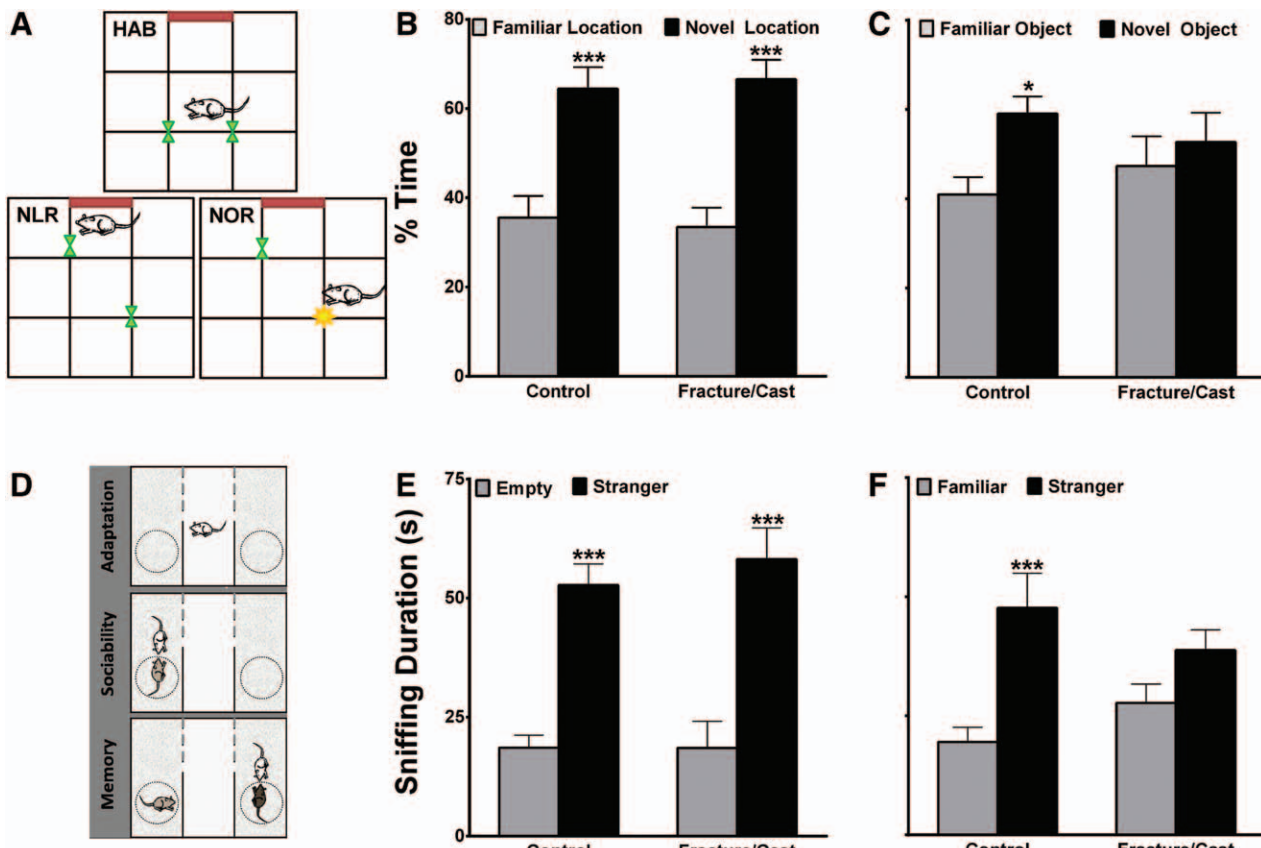


**Fig. 3.** Fracture/cast mice show signs of memory deficit. Schematic representation of the open field apparatus highlighting the habituation (HAB), novel location recognition (NLR), and novel object recognition (NOR) testing configurations (A). Fracture/cast mice do not differ from control mice in the time spent exploring the displaced object (B), but they do differ in the time spent exploring a novel object (C). Schematic representation of the social memory testing apparatus (D). Fracture/cast mice do not differ from control mice in the total time spent socializing with a stranger mouse (E); however, fracture/cast mice do not spend more time socializing with a newly introduced stranger (F). \* $P < 0.05$ , \*\*\* $P < 0.001$ . n = 16 per group. Errors bars = SEM.

show increased complexity in dendritic structure in the contralateral amygdala, as shown by the mean number of intersections of dendritic branches with consecutive 5- $\mu\text{m}$ -spaced concentric Sholl rings (fig. 4A; individual two-tailed  $t$  tests with Holm–Sidak correction for multiple comparisons; area under the curve comparison: two-tailed  $t$  test,  $238.5 \pm 13.92$  in control vs.  $404.1 \pm 28.47$  in fracture/cast mice,  $P = 0.01$ ). Furthermore, independent quantification of neuronal structure using direct counts revealed that the fracture/cast group has a significantly greater number of secondary nodes compared with control, indicative of increased dendritic branching (fig. 4B; two-tailed  $t$  test,  $1.31 \pm 0.12$  in control vs.  $2.75 \pm 0.35$  in fracture/cast mice,  $P = 0.01$ ). No differences were seen in measures of dendritic length (fig. 4C; two-tailed  $t$  test,  $243.7 \pm 15.08$   $\mu\text{m}$  in control vs.  $403.7 \pm 77.79$   $\mu\text{m}$  in fracture/cast mice,  $P = 0.09$ , [Welch's correction applied]), average soma area (fig. 4D; two-tailed  $t$  test,  $108.2 \pm 6.75$   $\mu\text{m}^2$  in control vs.  $109.5 \pm 7.43$   $\mu\text{m}^2$  in fracture/cast mice,  $P = 0.9$ ), total number of neurons (fig. 4E; two-tailed  $t$  test,  $29.2 \pm 1.24$  in control vs.  $30.71 \pm 2.81$  in fracture/cast mice,  $P = 0.67$ ),

or dendritic spine density (fig. 4, F and G; two-tailed  $t$  test,  $12.96 \pm 0.96$  in control vs.  $11.86 \pm 1.11$  in fracture/cast mice,  $P = 0.49$ ).

#### Fracture/Cast Animals Show Altered Dendritic Architecture in the Perirhinal Cortex

Similar to the results obtained in the amygdala, Sholl analysis revealed that, compared with control, fracture/cast mice show increased complexity in dendritic structure in the contralateral perirhinal cortex, as shown by the mean number of intersections of dendrite branches with concentrically spaced Sholl rings (fig. 5A; individual two-tailed  $t$  tests with Holm–Sidak correction for multiple comparisons; area under the curve comparison: two-tailed  $t$  test,  $304.9 \pm 32.33$  in control vs.  $416.6 \pm 23.83$  in fracture/cast mice,  $P = 0.02$ ). Independent quantification of neuronal structure revealed that the fracture/cast group has a significantly greater number of secondary nodes compared with control, indicative of increased dendritic branching (fig. 5B; two-tailed  $t$  test,  $1.62 \pm 0.04$  in control vs.  $2.57 \pm 0.29$  in fracture/cast mice,  $P = 0.03$ , [Welch's correction applied]). Furthermore, total dendritic length was shown to be greater in fracture/cast

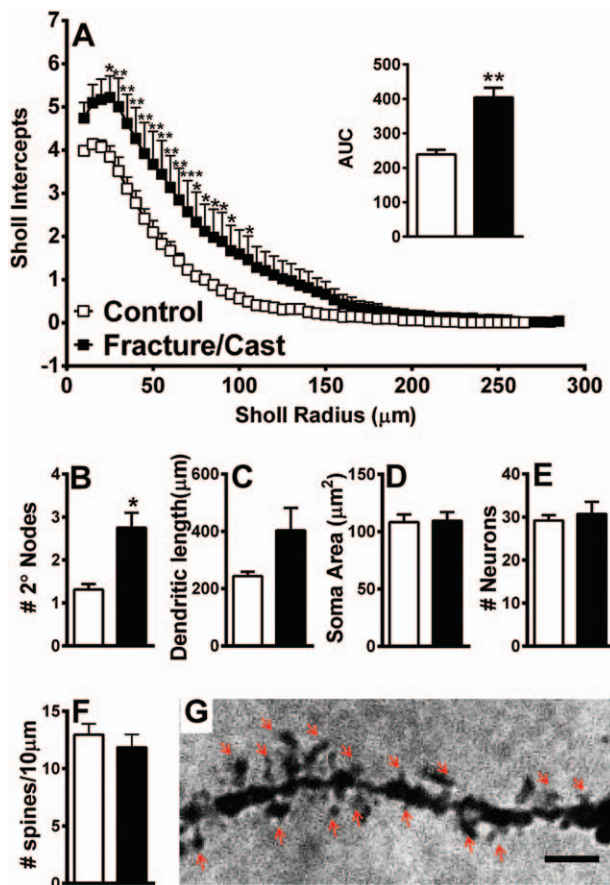


**Fig. 4.** Dendritic architecture is changed in the amygdala of fracture/cast mice. Fracture/cast mice display increased dendritic complexity in the amygdala as shown by the mean number of intersections of dendrite branches with consecutive 5-μm-spaced concentric Sholl rings (A) and by calculating the area under the curve (AUC) for these two curves (A, inset). In addition, the fracture group has a significantly greater number of secondary nodes compared with control (B). No differences were seen in measures of total dendritic length (C), average soma area (D), total number of neurons (E), or dendritic spine density (F, G). Scale bar = 1 μm. \*P < 0.05, \*\*P < 0.01. n = 5 (control) and n = 7 (fracture/cast). Errors bars = SEM. Red arrows point to dendritic spines.

mice (fig. 5C; two-tailed *t* test,  $280.4 \pm 12.69$  μm in control *vs.*  $471.5 \pm 41.23$  μm in fracture/cast mice, *P* = 0.003, [Welch's correction applied]). No differences were seen in average soma area (fig. 5D; two-tailed *t* test,  $205.3 \pm 15.23$  μm<sup>2</sup> in control *vs.*  $242.2 \pm 20.7$  μm<sup>2</sup> in fracture/cast mice, *P* = 0.2), total number of neurons (fig. 5E; two-tailed *t* test,  $17.2 \pm 0.80$  in control *vs.*  $14.43 \pm 1.9$  in fracture/cast mice, *P* = 0.27), or dendritic spine density (fig. 5, F and G; two-tailed *t* test,  $18.04 \pm 1.4$  in control *vs.*  $19.32 \pm 0.71$  in fracture per cast mice, *P* = 0.2).

#### Fracture/Cast Animals Show No Obvious Changes in Dendritic Morphology in the Hippocampus

Unlike the amygdala and the perirhinal cortex, dendritic analysis was not undertaken in the hippocampus due to

high-dendrite density. Instead, the number of neurons and the dendritic spine density were quantified. Our results show no significant change in the number of neurons (fig. 6A; two-tailed *t* test,  $37.4 \pm 2.06$  in control *vs.*  $39.5 \pm 3.96$  in fracture/cast mice, *P* = 0.67) or dendritic spines (fig. 6, B and C; two-tailed *t* test,  $13.88 \pm 1.87$  in control *vs.*  $10.8 \pm 0.99$  in fracture per cast mice, *P* = 0.07).

#### Fracture/Cast Animals Show Decreased Levels of Synaptophysin in the Hippocampus

To complement the dendritic morphology analysis, we measured synaptophysin levels in synaptosomal preparations from the following brain regions: amygdala, perirhinal cortex, and hippocampus. Our results reveal that, despite our prior findings showing increased dendritic branching in the amygdala and perirhinal cortex, synaptophysin levels remained unchanged (compared to control) in both regions (fig. 7A; two-tailed *t* test,  $1.53 \pm 0.15$  in control *vs.*  $1.16 \pm 0.19$  in fracture per cast mice, *P* = 0.21; fig. 7B; two-tailed *t* test,  $2.82 \pm 0.86$  in control *vs.*  $2.13 \pm 0.22$  in fracture per cast mice, *P* = 0.26). In the hippocampus, however, the fracture mice exhibited decreased levels of synaptophysin, indicative of a reduction in the number of synapses<sup>35</sup> (fig. 7C; two-tailed *t* test,  $2.82 \pm 0.58$  in control *vs.*  $1.01 \pm 0.07$  in fracture per cast mice, *P* = 0.001).

#### Fracture/Cast Animals Show Decreased BDNF Levels in the Perirhinal Cortex and Hippocampus

To test whether these morphological/synaptic changes are paralleled by changes in neurotrophic factors, we measured BDNF levels using ELISA. Our data show that, in the amygdala, fracture/cast and control mice show similar levels of BDNF (fig. 8A; two-tailed *t* test,  $1,076 \pm 106$  ng/g in control *vs.*  $1,142 \pm 30.55$  ng/g in fracture/cast mice, *P* = 0.76). In contrast, compared with control mice, fracture/cast mice display decreased levels of BDNF in the perirhinal cortex (fig. 8B; two-tailed *t* test,  $1,398 \pm 66.53$  ng/g in control *vs.*  $959.6 \pm 82.58$  ng/g in fracture/cast mice, *P* = 0.006) and the hippocampus (fig. 8C; two-tailed *t* test,  $7,312 \pm 346.3$  ng/g in control *vs.*  $6,335 \pm 214.6$  ng/g in fracture/cast mice, *P* = 0.03).

## Discussion

Although pain itself is the most common complaint of the chronic pain patient, it is often associated with comorbid conditions such as cognitive impairment,<sup>36</sup> memory deficits,<sup>37</sup> depression,<sup>38</sup> and anxiety.<sup>39,40</sup> These affect up to 50% of chronic pain patients<sup>11,41,42</sup> and impair both quality of life and response to treatment.<sup>43</sup> In addition, CRPS patients reportedly demonstrate diminished capacity for tactile perceptual learning<sup>44</sup> and altered performance in a gambling task, implying changes in emotional influences on decision making and risk taking.<sup>45</sup> Neuropsychiatric testing on a group of 137 CRPS patients revealed deficits in 65% of patients, including subgroups having deficits in executive functioning, memory, and even global cognitive

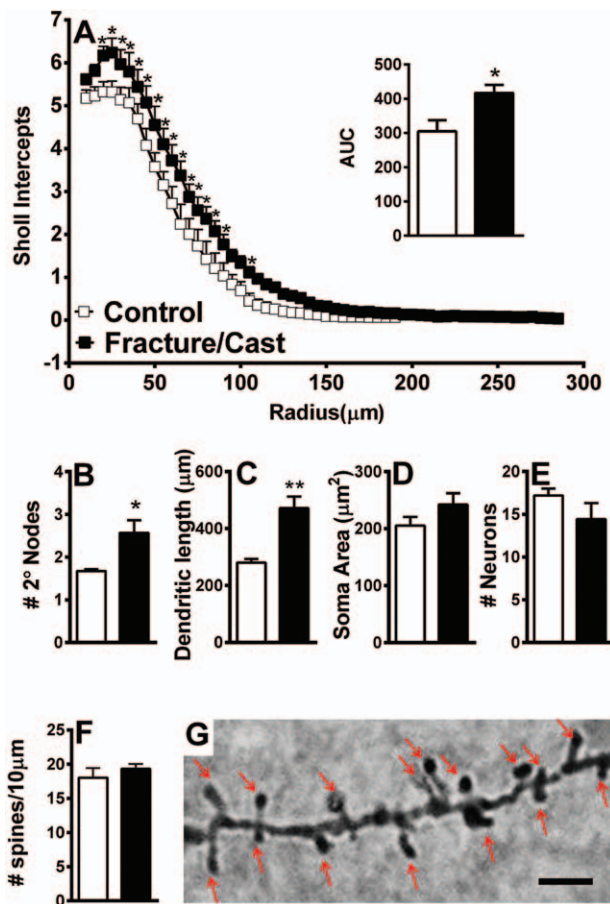


**Fig. 5.** Dendritic architecture is changed in the perirhinal cortex of fracture/cast mice. Cast/fracture mice display increased dendritic complexity in the perirhinal cortex as shown by the mean number of intersections of dendrite branches with consecutive 5-μm-spaced concentric Sholl rings (A) and by calculating the area under the curve (AUC) for these two curves (A, inset). In addition, the fracture group has a significantly greater number of secondary nodes compared with control (B) and a greater average of total dendritic length (C). No differences were observed in average soma area (D), total number of neurons (E), or dendritic spine density (F, G). Scale bar = 1 μm. \*P < 0.05, \*\*P < 0.01. n = 5 (control) and n = 7 (fracture/cast). Errors bars = SEM. Red arrows point to dendritic spines.

impairment.<sup>46</sup> Furthermore, psychological factors such as depression and anxiety are strongly associated with CRPS severity.<sup>47,48</sup> Taken together, these data emphasize that cognitive and affective impairments are significant clinical problems in chronic CRPS.

Although most preclinical pain studies focus on mechanical sensitivity as the primary outcome, there has been increasing interest in the affective measures of pain and its associated comorbidities. For instance, there is evidence of anxiety<sup>49,50</sup> and attention deficits<sup>51–55</sup> in rodent models of pain, in addition to changes in mood<sup>50,56,57</sup> and overall cognitive function.<sup>58–60</sup> Similar to what is seen in patients,<sup>61</sup> some of these conditions subside once the pain is ameliorated.<sup>62</sup> We have

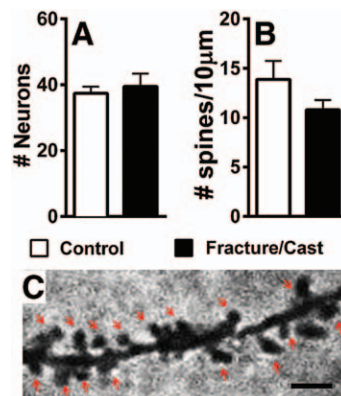


**Fig. 6.** No obvious dendritic changes in the hippocampus of fracture/cast mice. Fracture/cast mice do not differ in the number of neurons (A) or dendritic spine density (B, C) in the hippocampus. Scale bar = 1 μm. n = 5 (control) and n = 7 (fracture/cast). Errors bars = SEM. Red arrows point to dendritic spines.

shown that selective signs of neophobic anxiety (in the form of altered thigmotaxis in the zero maze but not OF assay) and memory impairment (NOR and social memory but not NLR) are present in our fracture/cast mice.

What, then, is the neurobiological substrate of these behavioral changes? With the advent of noninvasive brain imaging techniques, we now have evidence of structural and functional brain changes directly associated with the pain experience in chronic neuropathy,<sup>63,64</sup> fibromyalgia,<sup>48,65</sup> migraine,<sup>66</sup> chronic back pain<sup>67–69</sup>, and CRPS.<sup>70</sup> Although such studies have given us invaluable insight into the “pain” brain, there remains a need for a more detailed analysis of neuroplasticity in the affected areas. Based on our behavioral observations, we focused on three potential neurobiological substrates. The amygdala was chosen based on its role in processing threatening stimuli,<sup>20</sup> mood,<sup>21</sup> fear,<sup>71</sup> emotional memory,<sup>22</sup> anxiety,<sup>72,73</sup> and the emotional-affective dimension of pain.<sup>74</sup> The perirhinal cortex and hippocampus were chosen for their roles in memory. The participation of the hippocampus in memory has been described extensively (e.g., see the study by Gerlai<sup>75</sup> and Broadbent *et al.*<sup>76</sup>) and can be studied using paradigms such as novel object location and social memory.<sup>77</sup> There is accumulating evidence for the role of the perirhinal cortex in memory as well. Studies in humans, monkeys, and rodents suggest that this area is involved in signaling the familiarity of objects,<sup>78</sup> in particular, NOR<sup>23,79</sup> and this may take place in a hippocampus-independent manner.<sup>24,78</sup> It is noteworthy that, despite attributing certain behavioral outcomes to respective brain regions, there is considerable overlap between the roles that these regions play.<sup>80</sup>

One of the mechanisms of modulating synaptic plasticity is the differential localization of specific synaptic sites. As such, analysis of dendritic structure, morphology, length, and arborization, in addition to quantification of spine density and levels of BDNF and the presynaptic protein synaptophysin are indicators of ongoing neural plasticity. Our

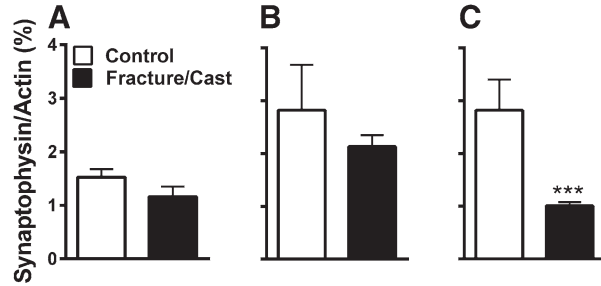


**Fig. 7.** Decreased synaptophysin in the hippocampus of fracture/cast mice. Compared with control mice, fracture/cast mice do not show differences in the levels of synaptophysin in the amygdala (A) or the perirhinal cortex (B). However, they do display decreased levels of synaptophysin in the hippocampus (C) measured by western blots of the synaptosomal preparation. \*\*\* $P < 0.001$ . n = 5 (control) and n = 7 (fracture/cast). Errors bars = SEM.

behavioral observations of increased anxiety-related behaviors in the zero maze, impairment in NOR, and impairment in social memory were paralleled by changes in the dendritic architecture of the amygdala and perirhinal cortex where data from our Golgi-Cox-stained sections showed increased dendritic branching and length in CRPS mice, without any changes in soma size. This is consistent with previous findings where dendritic architecture in the anterior cingulate cortex, somatosensory cortex, and dorsal horn spinal cord neurons is altered in rodent pain models,<sup>81,82</sup> with the notable difference that dendritic spine density was not shown to change in our model. Remarkably, increased dendritic complexity is also associated with enriched environments,<sup>83</sup> implying that these changes are not necessarily maladaptive in all cases. In the current study, dendritic analysis was not undertaken in the hippocampus due to the high-dendrite density in that region making the Golgi-Cox-stained patterns difficult to analyze. Instead, quantification of spine density was carried out and revealed no statistically significant change in dendritic spine number. Furthermore, no change in the number of newborn neurons was observed between the fracture/cast and control group in this region (data not shown).

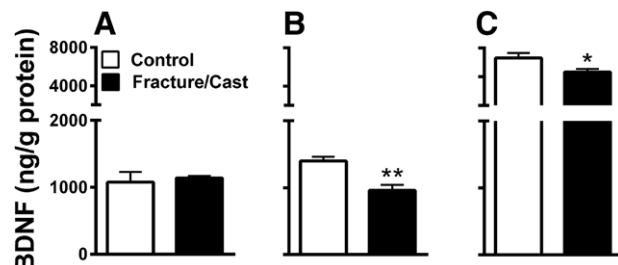


**Fig. 8.** Decreased brain-derived neurotrophic factor (BDNF) in the perirhinal cortex and hippocampus of fracture/cast mice. Fracture/cast mice do not differ from control in the levels of BDNF protein in the amygdala (A). However, they do display decreased levels of BDNF in the perirhinal cortex (B) and the hippocampus (C). \* $P < 0.05$ , \*\* $P < 0.01$ . n = 5 (control) and n = 7 (fracture/cast). Errors bars = SEM.

The dendritic architecture of a neuron is critical in determining the number and type of synaptic connections possessed by that neuron in addition to governing how synaptic inputs are integrated to produce a coded output. We therefore examined whether synaptic abundance parallels the increased dendritic branching. Our findings show that the histological changes indicative of increased dendritic complexity occur in the amygdala and perirhinal cortex in the absence of increased synaptophysin, an indirect measure of synaptic numbers.<sup>35</sup> Furthermore, synaptophysin levels are decreased in hippocampi isolated from CRPS mice, and trended toward lower levels in homogenates of tissue from the perirhinal cortex and amygdala. These data agree with our histological measures of spine density. It is possible that although CRPS brains display patterns of increased dendritic branching, they do not necessarily form more synapses compared with control mice, a hypothesis that is consistent with the anxiety and memory deficits observed in this model. Alternatively, it is possible that dendritic branching is a consequence of, or compensation for, synaptic loss. These data are in agreement with earlier findings showing that decreased levels of synaptophysin are accompanied by impairment in cognitive function and memory<sup>84</sup> and *vice versa*.<sup>85</sup> In contrast, some brain regions (such as the prefrontal cortex) display increased levels of synaptic proteins,<sup>86</sup> including synaptophysin,<sup>87</sup> after chronic painful conditions.

Finally, brain plasticity can be assessed by quantifying levels of neurotrophins such as BDNF. BDNF is a potent modulator of synaptic plasticity,<sup>88,89</sup> due at least in part to colocalization with its cognate receptor TrkB at glutamatergic synapses.<sup>90</sup> The role of BDNF in pain has been extensively studied in preclinical models at the spinal level, and increased spinal BDNF is thought to contribute to central sensitization.<sup>91</sup> In addition, levels of BDNF increase in the periaqueductal gray and rostral ventromedial medulla in animal models of pain, possibly contributing to descending pain facilitation.<sup>92</sup> In contrast, BDNF is decreased in the hippocampus after painful stimuli,<sup>93,94</sup> but its levels have not been measured in the more chronic stages of pain, where comorbidities often appear. We observed a significant decrease in BDNF levels in the perirhinal cortex and hippocampus in agreement with other rodent studies where depression and anxiety/stress are associated with signs of memory impairment<sup>95</sup> and decreased levels of BDNF in the hippocampus.<sup>96,97</sup> Finally, our findings failed to show changes in BDNF levels in the amygdala, despite previous studies linking increased BDNF to stress and trauma.<sup>98</sup> It is possible that a more careful examination of the subregions of the amygdala is needed to address this disparity. Alternatively, it is possible that anxiety levels in our fracture/cast mice (detectable by zero maze and not OF) are not “high” enough to be associated with BDNF changes.

We believe that the approach of measuring neurocognitive and affective components of pain in conjunction with

neuroplastic CNS changes in models such as the fracture/cast animals is crucial in understanding the multifaceted nature of chronic pain. In this way, we will build a “language of translation,” helping us to focus mechanistically oriented animal studies on regions of the CNS implicated in human studies, and perhaps to focus human studies on approaches to treatment or prevention of the CNS changes that are optimized using animal models.

There are several limitations to the present set of studies. For example, we focused only on the hippocampus, amygdala, and perirhinal cortex. Although these regions are involved in anxiety and memory, areas such as the prefrontal cortex, the somatosensory cortex, and the thalamus are also important to examine since each of these has been associated with brain changes in preclinical models of pain<sup>99</sup> and in chronic pain patients.<sup>48,67,100</sup> In addition, we have not identified any of the specific mechanisms linking peripheral injury and immobilization with the CNS changes. Future studies examining the molecular underpinnings of the fracture/cast-related changes in the brain, perhaps with particular emphasis on epigenetic changes, are needed. Epigenetic mechanisms are well suited to modulate the long-lasting CNS changes that accompany chronic pain.<sup>86,99,101</sup>

Collectively, these data provide unique evidence for structural and biochemical changes in the brain that accompany selective measures of anxiety (changes in thigmotactic behaviors in the zero maze but not the OF assay) and working memory (NOR but not NLR) and social memory impairment in a mouse model of tibia fracture/cast immobilization. These findings have clear clinical implications for the CRPS patient, since, in addition to elucidating some of the supraspinal correlates of the syndrome, this work supports the potential use of therapeutic interventions that not only directly target sensory input and other peripheral mechanisms, but also attempt to ameliorate the pain experience by modifying its associated cognitive and emotional comorbidities.

## Acknowledgments

The authors thank Frances Davies, Ph.D. (Palo Alto Institute of Research and Education, Palo Alto, California), for technical assistance.

This study was supported by the National Institutes of Health (Bethesda, Maryland; grant no. NS072168 to Drs. Kingery and Clark) and by the Department of Veterans Affairs (Palo Alto, California) merit review grant (to Dr. Huang).

## Competing Interests

The authors declare no competing interests.

## Correspondence

Address correspondence to Dr. Tajerian: Anesthesia Service, Veterans Affairs Palo Alto Health Care System, 3801 Miranda Avenue, Palo Alto, California 94304. maral@stanford.edu. Information on purchasing reprints may be found at [www.anesthesiology.org](http://www.anesthesiology.org) or on the masthead page at the beginning of this issue. ANESTHESIOLOGY's articles are made freely

accessible to all readers, for personal use only, 6 months from the cover date of the issue.

## References

1. de Mos M, de Brujin AG, Huygen FJ, Dieleman JP, Stricker BH, Sturkenboom MC: The incidence of complex regional pain syndrome: A population-based study. *Pain* 2007; 129:12–20
2. Goebel A: Complex regional pain syndrome in adults. *Rheumatology (Oxford)* 2011; 50:1739–50
3. Birklein F, Riedl B, Sieweke N, Weber M, Neundörfer B: Neurological findings in complex regional pain syndromes—Analysis of 145 cases. *Acta Neurol Scand* 2000; 101:262–9
4. Sieweke N, Birklein F, Riedl B, Neundörfer B, Handwerker HO: Patterns of hyperalgesia in complex regional pain syndrome. *Pain* 1999; 80:171–7
5. Cossins L, Okell RW, Cameron H, Simpson B, Poole HM, Goebel A: Treatment of complex regional pain syndrome in adults: A systematic review of randomized controlled trials published from June 2000 to February 2012. *Eur J Pain* 2013; 17:158–73
6. Dirckx M, Stronks DL, Groeneweg G, Huygen FJ: Effect of immunomodulating medications in complex regional pain syndrome: A systematic review. *Clin J Pain* 2012; 28:355–63
7. Subbarao J, Stillwell GK: Reflex sympathetic dystrophy syndrome of the upper extremity: Analysis of total outcome of management of 125 cases. *Arch Phys Med Rehabil* 1981; 62:549–54
8. Harden RN, Bruehl S, Perez RS, Birklein F, Marinus J, Maihofner C, Lubenow T, Buvanendran A, Mackey S, Graciosa J, Mogilevski M, Ramsden C, Schlereth T, Chont M, Vatine JJ: Development of a severity score for CRPS. *Pain* 2010; 151:870–6
9. Lohnberg JA, Altmaier EM: A review of psychosocial factors in complex regional pain syndrome. *J Clin Psychol Med Settings* 2013; 20:247–54
10. Berryman C, Stanton TR, Jane Bowering K, Tabor A, McFarlane A, Lorimer Moseley G: Evidence for working memory deficits in chronic pain: A systematic review and meta-analysis. *Pain* 2013; 154:1181–96
11. Landrø NI, Fors EA, Våpenstad LL, Holthe Ø, Stiles TC, Borchgrevink PC: The extent of neurocognitive dysfunction in a multidisciplinary pain centre population. Is there a relation between reported and tested neuropsychological functioning? *Pain* 2013; 154:972–7
12. Linnman C, Becerra L, Borsook D: Inflaming the brain: CRPS a model disease to understand neuroimmune interactions in chronic pain. *J Neuroimmune Pharmacol* 2013; 8:547–63
13. Schwenkreis P, Maier C, Tegenthoff M: Functional imaging of central nervous system involvement in complex regional pain syndrome. *AJR Am J Neuroradiol* 2009; 30:1279–84
14. Coderre TJ, Xanthos DN, Francis L, Bennett GJ: Chronic post-ischemia pain (CPIP): A novel animal model of complex regional pain syndrome-type I (CRPS-I; reflex sympathetic dystrophy) produced by prolonged hindpaw ischemia and reperfusion in the rat. *Pain* 2004; 112:94–105
15. Siegel SM, Lee JW, Oaklander AL: Needlestuck distal nerve injury in rats models symptoms of complex regional pain syndrome. *Anesth Analg* 2007; 105:1820–9
16. Bove GM: Focal nerve inflammation induces neuronal signs consistent with symptoms of early complex regional pain syndromes. *Exp Neurol* 2009; 219:223–7
17. Guo TZ, Offley SC, Boyd EA, Jacobs CR, Kingery WS: Substance P signaling contributes to the vascular and nociceptive abnormalities observed in a tibial fracture rat model of complex regional pain syndrome type I. *Pain* 2004; 108:95–107
18. Guo TZ, Wei T, Shi X, Li WW, Hou S, Wang L, Tsujikawa K, Rice KC, Cheng K, Clark DJ, Kingery WS: Neuropeptide

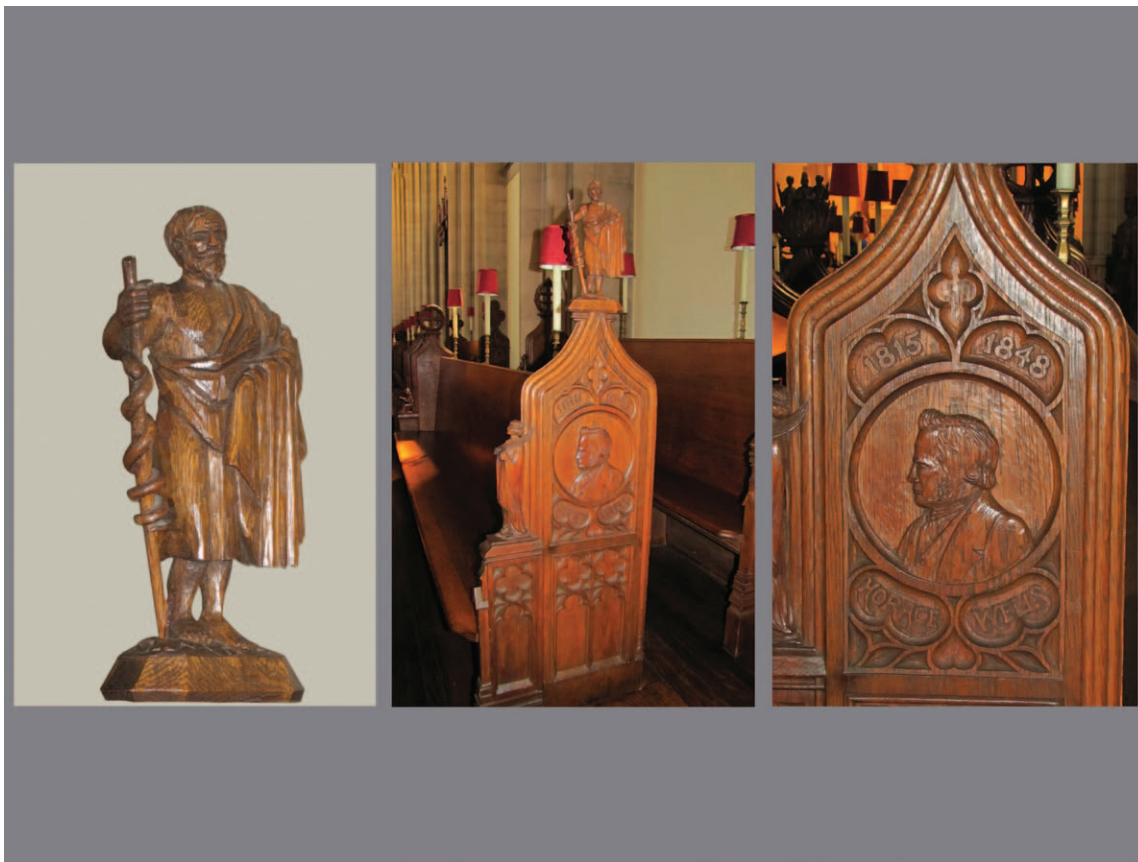
- deficient mice have attenuated nociceptive, vascular, and inflammatory changes in a tibia fracture model of complex regional pain syndrome. *Mol Pain* 2012; 8:85
19. Gallagher JJ, Tajerian M, Guo T, Shi X, Li W, Zheng M, Peltz G, Kingery WS, Clark JD: Acute and chronic phases of complex regional pain syndrome in mice are accompanied by distinct transcriptional changes in the spinal cord. *Mol Pain* 2013; 9:40
  20. Tasan RO, Nguyen NK, Weger S, Sartori SB, Singewald N, Heilbronn R, Herzog H, Sperk G: The central and basolateral amygdala are critical sites of neuropeptide Y/Y2 receptor-mediated regulation of anxiety and depression. *J Neurosci* 2010; 30:6282–90
  21. Seymour B, Dolan R: Emotion, decision making, and the amygdala. *Neuron* 2008; 58:662–71
  22. Phelps EA, LeDoux JE: Contributions of the amygdala to emotion processing: From animal models to human behavior. *Neuron* 2005; 48:175–87
  23. Mumby DG, Glenn MJ, Nesbitt C, Kyriazis DA: Dissociation in retrograde memory for object discriminations and object recognition in rats with perirhinal cortex damage. *Behav Brain Res* 2002; 132:215–26
  24. Barker GR, Warburton EC: When is the hippocampus involved in recognition memory? *J Neurosci* 2011; 31:10721–31
  25. Terkelsen AJ, Bach FW, Jensen TS: Experimental forearm immobilization in humans induces cold and mechanical hyperalgesia. *ANESTHESIOLOGY* 2008; 109:297–307
  26. Chaplan SR, Bach FW, Pogrel JW, Chung JM, Yaksh TL: Quantitative assessment of tactile allodynia in the rat paw. *J Neurosci Methods* 1994; 53:55–63
  27. Prut L, Belzung C: The open field as a paradigm to measure the effects of drugs on anxiety-like behaviors: A review. *Eur J Pharmacol* 2003; 463:3–33
  28. Shepherd JK, Grewal SS, Fletcher A, Bill DJ, Dourish CT: Behavioural and pharmacological characterisation of the elevated “zero-maze” as an animal model of anxiety. *Psychopharmacology (Berl)* 1994; 116:56–64
  29. Mumby DG, Gaskin S, Glenn MJ, Schramek TE, Lehmann H: Hippocampal damage and exploratory preferences in rats: Memory for objects, places, and contexts. *Learn Mem* 2002; 9:49–57
  30. DeLorey TM, Sahbaie P, Hashemi E, Homanics GE, Clark JD: Gabrb3 gene deficient mice exhibit impaired social and exploratory behaviors, deficits in non-selective attention and hypoplasia of cerebellar vermal lobules: A potential model of autism spectrum disorder. *Behav Brain Res* 2008; 187:207–20
  31. Inta D, Vogt MA, Perreau-Lenz S, Schneider M, Pfeiffer N, Wojcik SM, Spanagel R, Gass P: Sensorimotor gating, working and social memory deficits in mice with reduced expression of the vesicular glutamate transporter VGLUT1. *Behav Brain Res* 2012; 228:328–32
  32. Jamain S, Radyushkin K, Hammerschmidt K, Granon S, Boretius S, Varoqueaux F, Ramanantsoa N, Gallego J, Ronnenberg A, Winter D, Frahm J, Fischer J, Bourgeron T, Ehrenreich H, Brose N: Reduced social interaction and ultrasonic communication in a mouse model of monogenic heritable autism. *Proc Natl Acad Sci U S A* 2008; 105:1710–5
  33. Paxinos G, Franklin KBJ, Franklin KBJ: The Mouse Brain in Stereotaxic Coordinates, 2nd edition. San Diego, Academic Press, 2001
  34. Kim BG, Dai HN, McAtee M, Vicini S, Bregman BS: Remodeling of synaptic structures in the motor cortex following spinal cord injury. *Exp Neurol* 2006; 198:401–15
  35. Calhoun ME, Jucker M, Martin LJ, Thinakaran G, Price DL, Mouton PR: Comparative evaluation of synaptophysin-based methods for quantification of synapses. *J Neurocytol* 1996; 25:821–8
  36. McCracken LM, Iverson GL: Predicting complaints of impaired cognitive functioning in patients with chronic pain. *J Pain Symptom Manage* 2001; 21:392–6
  37. Schnurr RF, MacDonald MR: Memory complaints in chronic pain. *Clin J Pain* 1995; 11:103–11
  38. Fishbain DA, Cutler R, Rosomoff HL, Rosomoff RS: Chronic pain-associated depression: Antecedent or consequence of chronic pain? A review. *Clin J Pain* 1997; 13:116–37
  39. Dersh J, Polatin PB, Gatchel RJ: Chronic pain and psychopathology: Research findings and theoretical considerations. *Psychosom Med* 2002; 64:773–86
  40. McWilliams LA, Cox BJ, Enns MW: Mood and anxiety disorders associated with chronic pain: An examination in a nationally representative sample. *Pain* 2003; 106:127–33
  41. Geisser ME, Roth RS, Robinson ME: Assessing depression among persons with chronic pain using the Center for Epidemiological Studies-Depression Scale and the Beck Depression Inventory: A comparative analysis. *Clin J Pain* 1997; 13:163–70
  42. Gerrits MM, van Oppen P, van Marwijk HW, Penninx BW, van der Horst HE: Pain and the onset of depressive and anxiety disorders. *Pain* 2014; 155:53–9
  43. Bromley Milton M, Börsbo B, Rovner G, Lundgren-Nilsson A, Stibrant-Sunnerhagen K, Gerdle B: Is pain intensity really that important to assess in chronic pain patients? A study based on the Swedish Quality Registry for Pain Rehabilitation (SQRP). *PLoS One* 2013; 8:e65483
  44. Maihofner C, DeCol R: Decreased perceptual learning ability in complex regional pain syndrome. *Eur J Pain* 2007; 11:903–9
  45. Apkarian AV, Sosa Y, Krauss BR, Thomas PS, Fredrickson BE, Levy RE, Harden RN, Chialvo DR: Chronic pain patients are impaired on an emotional decision-making task. *Pain* 2004; 108:129–36
  46. Libon DJ, Schwartzman RJ, Eppig J, Wambach D, Brahin E, Peterlin BL, Alexander G, Kalanuria A: Neuropsychological deficits associated with Complex Regional Pain Syndrome. *J Int Neuropsychol Soc* 2010; 16:566–73
  47. Kim SK, Eto K, Nabekura J: Synaptic structure and function in the mouse somatosensory cortex during chronic pain: *In vivo* two-photon imaging. *Neural Plast* 2012; 2012:640259
  48. Jensen KB, Loitoile R, Kosek E, Petzke F, Carville S, Fransson P, Marcus H, Williams SC, Choy E, Mainguy Y, Vitton O, Gracely RH, Gollub R, Ingvar M, Kong J: Patients with fibromyalgia display less functional connectivity in the brain's pain inhibitory network. *Mol Pain* 2012; 8:32
  49. Chen J, Song Y, Yang J, Zhang Y, Zhao P, Zhu XJ, Su HC: The contribution of TNF- $\alpha$  in the amygdala to anxiety in mice with persistent inflammatory pain. *Neurosci Lett* 2013; 541:275–80
  50. Suzuki T, Amata M, Sakae G, Nishimura S, Inoue T, Shibata M, Mashimo T: Experimental neuropathy in mice is associated with delayed behavioral changes related to anxiety and depression. *Anesth Analg* 2007; 104:1570–7
  51. Low LA, Millecamp M, Seminowicz DA, Naso L, Thompson SJ, Stone LS, Bushnell MC: Nerve injury causes long-term attentional deficits in rats. *Neurosci Lett* 2012; 529:103–7
  52. Millecamp M, Etienne M, Jourdan D, Eschalier A, Ardid D: Decrease in non-selective, non-sustained attention induced by a chronic visceral inflammatory state as a new pain evaluation in rats. *Pain* 2004; 109:214–24
  53. Ford GK, Moriarty O, McGuire BE, Finn DP: Investigating the effects of distracting stimuli on nociceptive behaviour and associated alterations in brain monoamines in rats. *Eur J Pain* 2008; 12:970–9
  54. Boyette-Davis JA, Thompson CD, Fuchs PN: Alterations in attentional mechanisms in response to acute inflammatory pain and morphine administration. *Neuroscience* 2008; 151:558–63
  55. Pais-Vieira M, Lima D, Galhardo V: Sustained attention deficits in rats with chronic inflammatory pain. *Neurosci Lett* 2009; 463:98–102

56. Yalcin I, Bohren Y, Waltisperger E, Sage-Cioccia D, Yin JC, Freund-Mercier MJ, Barrot M: A time-dependent history of mood disorders in a murine model of neuropathic pain. *Biol Psychiatry* 2011; 70:946–53
57. Leitl MD, Onvani S, Bowers MS, Cheng K, Rice KC, Carlezon WA Jr, Banks ML, Negus SS: Pain-related depression of the mesolimbic dopamine system in rats: Expression, blockade by analgesics, and role of endogenous κ-opioids. *Neuropharmacology* 2014; 39:614–24
58. Kodama D, Ono H, Tanabe M: Increased hippocampal glycine uptake and cognitive dysfunction after peripheral nerve injury. *Pain* 2011; 152:809–17
59. Grégoire S, Michaud V, Chapuy E, Eschalier A, Ardid D: Study of emotional and cognitive impairments in mononeuropathic rats: Effect of duloxetine and gabapentin. *Pain* 2012; 153:1657–63
60. Ren WJ, Liu Y, Zhou LJ, Li W, Zhong Y, Pang RP, Xin WJ, Wei XH, Wang J, Zhu HQ, Wu CY, Qin ZH, Liu G, Liu XG: Peripheral nerve injury leads to working memory deficits and dysfunction of the hippocampus by upregulation of TNF-α in rodents. *Neuropharmacology* 2011; 36:979–92
61. Koffler SP, Hampstead BM, Irani F, Tinker J, Kiefer RT, Rohr P, Schwartzman RJ: The neurocognitive effects of 5 day anesthetic ketamine for the treatment of refractory complex regional pain syndrome. *Arch Clin Neuropsychol* 2007; 22:719–29
62. Vachon P, Millecamp M, Low L, Thompson SJ, Pailleux F, Beaudry F, Bushnell CM, Stone LS: Alleviation of chronic neuropathic pain by environmental enrichment in mice well after the establishment of chronic pain. *Behav Brain Funct* 2013; 9:22
63. Wu Q, Inman RD, Davis KD: Neuropathic pain in ankylosing spondylitis: A psychophysics and brain imaging study. *Arthritis Rheum* 2013; 65:1494–503
64. Widerström-Noga E, Pattany PM, Cruz-Almeida Y, Felix ER, Perez S, Cardenas DD, Martinez-Arizala A: Metabolite concentrations in the anterior cingulate cortex predict high neuropathic pain impact after spinal cord injury. *Pain* 2013; 154:204–12
65. Robinson ME, Craggs JG, Price DD, Perlstein WM, Staud R: Gray matter volumes of pain-related brain areas are decreased in fibromyalgia syndrome. *J Pain* 2011; 12:436–43
66. Messina R, Rocca MA, Colombo B, Valsasina P, Horsfield MA, Copetti M, Falini A, Comi G, Filippi M: Cortical abnormalities in patients with migraine: A surface-based analysis. *Radiology* 2013; 268:170–80
67. Apkarian AV, Sosa Y, Sonty S, Levy RM, Harden RN, Parrish TB, Gitelman DR: Chronic back pain is associated with decreased prefrontal and thalamic gray matter density. *J Neurosci* 2004; 24:10410–5
68. Schmidt-Wilcke T, Leinisch E, Gänssbauer S, Draganski B, Bogdahn U, Altmeppen J, May A: Affective components and intensity of pain correlate with structural differences in gray matter in chronic back pain patients. *Pain* 2006; 125:89–97
69. Seminowicz DA, Wideman TH, Naso L, Hatami-Khoroushahi Z, Fallatah S, Ware MA, Jarzem P, Bushnell MC, Shir Y, Ouellet JA, Stone LS: Effective treatment of chronic low back pain in humans reverses abnormal brain anatomy and function. *J Neurosci* 2011; 31:7540–50
70. Mutso AA, Radzicki D, Baliki MN, Huang L, Banisadr G, Centeno MV, Radulovic J, Martina M, Miller RJ, Apkarian AV: Abnormalities in hippocampal functioning with persistent pain. *J Neurosci* 2012; 32:5747–56
71. Pape HC, Pare D: Plastic synaptic networks of the amygdala for the acquisition, expression, and extinction of conditioned fear. *Physiol Rev* 2010; 90:419–63
72. Padival MA, Blume SR, Rosenkranz JA: Repeated restraint stress exerts different impact on structure of neurons in the lateral and basal nuclei of the amygdala. *Neuroscience* 2013; 246:230–42
73. Qin M, Xia Z, Huang T, Smith CB: Effects of chronic immobilization stress on anxiety-like behavior and basolateral amygdala morphology in Fmr1 knockout mice. *Neuroscience* 2011; 194:282–90
74. Neugebauer V, Li W, Bird GC, Han JS: The amygdala and persistent pain. *Neuroscientist* 2004; 10:221–34
75. Gerlai R: Behavioral tests of hippocampal function: Simple paradigms complex problems. *Behav Brain Res* 2001; 125:269–77
76. Broadbent NJ, Squire LR, Clark RE: Spatial memory, recognition memory, and the hippocampus. *Proc Natl Acad Sci U S A* 2004; 101:14515–20
77. Kogan JH, Frankland PW, Silva AJ: Long-term memory underlying hippocampus-dependent social recognition in mice. *Hippocampus* 2000; 10:47–56
78. Ranganath C, Ritchey M: Two cortical systems for memory-guided behaviour. *Nat Rev Neurosci* 2012; 13:713–26
79. Baxter MG, Murray EA: Opposite relationship of hippocampal and rhinal cortex damage to delayed nonmatching-to-sample deficits in monkeys. *Hippocampus* 2001; 11:61–71
80. Deacon RM, Bannerman DM, Rawlins JN: Anxiolytic effects of cytotoxic hippocampal lesions in rats. *Behav Neurosci* 2002; 116:494–7
81. Tan AM, Samad OA, Fischer TZ, Zhao P, Persson AK, Waxman SG: Maladaptive dendritic spine remodeling contributes to diabetic neuropathic pain. *J Neurosci* 2012; 32:6795–807
82. Xiao X, Yang Y, Zhang Y, Zhang XM, Zhao ZQ, Zhang YQ: Estrogen in the anterior cingulate cortex contributes to pain-related aversion. *Cereb Cortex* 2013; 23:2190–203
83. Greenough WT, Volkmar FR: Pattern of dendritic branching in occipital cortex of rats reared in complex environments. *Exp Neurol* 1973; 40:491–504
84. Lassmann H, Weiler R, Fischer P, Bancher C, Jellinger K, Floor E, Danielczyk W, Seitelberger F, Winkler H: Synaptic pathology in Alzheimer's disease: Immunological data for markers of synaptic and large dense-core vesicles. *Neuroscience* 1992; 46:1–8
85. Ya BL, Liu WY, Ge F, Zhang YX, Zhu BL, Bai B: Dietary cholesterol alters memory and synaptic structural plasticity in young rat brain. *Neurol Sci* 2013; 34:1355–65
86. Alvarado S, Tajerian M, Millecamp M, Suderman M, Stone LS, Szyf M: Peripheral nerve injury is accompanied by chronic transcriptome-wide changes in the mouse prefrontal cortex. *Mol Pain* 2013; 9:21
87. Hung KL, Wang SJ, Wang YC, Chiang TR, Wang CC: Upregulation of presynaptic proteins and protein kinases associated with enhanced glutamate release from axonal terminals (synaptosomes) of the medial prefrontal cortex in rats with neuropathic pain. *Pain* 2014; 155:377–87
88. Schindler AF, Poo M: The neurotrophin hypothesis for synaptic plasticity. *Trends Neurosci* 2000; 23:639–45
89. Lu B: BDNF and activity-dependent synaptic modulation. *Learn Mem* 2003; 10:86–98
90. Bramham CR, Messaoudi E: BDNF function in adult synaptic plasticity: The synaptic consolidation hypothesis. *Prog Neurobiol* 2005; 76:99–125
91. Mannion RJ, Costigan M, Decosterd I, Amaya F, Ma QP, Holstege JC, Ji RR, Acheson A, Lindsay RM, Wilkinson GA, Woolf CJ: Neurotrophins: Peripherally and centrally acting modulators of tactile stimulus-induced inflammatory pain hypersensitivity. *Proc Natl Acad Sci U S A* 1999; 96:9385–90
92. Guo W, Robbins MT, Wei F, Zou S, Dubner R, Ren K: Supraspinal brain-derived neurotrophic factor signaling: A novel mechanism for descending pain facilitation. *J Neurosci* 2006; 26:126–37
93. Duric V, McCarron KE: Neurokinin-1 (NK-1) receptor and brain-derived neurotrophic factor (BDNF) gene expression is differentially modulated in the rat spinal dorsal horn and hippocampus during inflammatory pain. *Mol Pain* 2007; 3:32

94. Duric V, McC Carson KE: Persistent pain produces stress-like alterations in hippocampal neurogenesis and gene expression. *J Pain* 2006; 7:544–55
95. Patki G, Solanki N, Atrooz F, Allam F, Salim S: Depression, anxiety-like behavior and memory impairment are associated with increased oxidative stress and inflammation in a rat model of social stress. *Brain Res* 2013; 1539:73–86
96. Blugeot A, Rivat C, Bouvier E, Molet J, Mouchard A, Zeau B, Bernard C, Benoliel JJ, Becker C: Vulnerability to depression: From brain neuroplasticity to identification of biomarkers. *J Neurosci* 2011; 31:12889–99
97. Duric V, McC Carson KE: Hippocampal neurokinin-1 receptor and brain-derived neurotrophic factor gene expression is decreased in rat models of pain and stress. *Neuroscience* 2005; 133:999–1006
98. Bennett MR, Lagopoulos J: Stress and trauma: BDNF control of dendritic-spine formation and regression. *Prog Neurobiol* 2014; 112:80–99
99. Tajerian M, Alvarado S, Millecamps M, Vachon P, Crosby C, Bushnell MC, Szlyf M, Stone LS: Peripheral nerve injury is associated with chronic, reversible changes in global DNA methylation in the mouse prefrontal cortex. *PLoS One* 2013; 8:e55259
100. Linnman C, Becerra L, Lebel A, Berde C, Grant PE, Borsook D: Transient and persistent pain induced connectivity alterations in pediatric complex regional pain syndrome. *PLoS One* 2013; 8:e57205
101. Uchida H, Matsushita Y, Ueda H: Epigenetic regulation of BDNF expression in the primary sensory neurons after peripheral nerve injury: Implications in the development of neuropathic pain. *Neuroscience* 2013; 240:147–54

## ANESTHESIOLOGY REFLECTIONS FROM THE WOOD LIBRARY-MUSEUM

### The Horace Wells Pew in Trinity College Chapel



In 1937 in Hartford, Connecticut, the Horace Wells Club presented a pew to Trinity College Chapel to memorialize the dentist who popularized the anesthetic use of nitrous oxide, Dr. Horace Wells. A profile bust of Wells (*right*) is carved between pairs of dental silhouettes, “Horace” and “Wells” beneath and his years of life above, from “1815” to “1848.” Wells’ portrait faces a carved figure (*middle*) of Saint Apollonia, the martyred patron saint of dentistry. A carving of Asklepios (Aesculapius), the ancient Greek god of medicine, tops (*left*) this end of the pew. (Copyright © the American Society of Anesthesiologists, Inc.)

*George S. Bause, M.D., M.P.H., Honorary Curator, ASA's Wood Library-Museum of Anesthesiology, Schaumburg, Illinois, and Clinical Associate Professor, Case Western Reserve University, Cleveland, Ohio. UJYC@aol.com.*